Structure and morphology of sol–gel prepared polymer–ceramic composite thin films

Frank W. Embs and Edwin L. Thomas*
Materials Science and Engineering Department, Massachusetts Institute of Technology, Cambridge, MA 02139, USA

and Chichang J. Wung† and Paras N. Prasad
Photonics Research Laboratory, Department of Chemistry, State University of New York at Buffalo, Buffalo, NY 14214, USA
(Received 17 August 1992; revised 5 March 1993)

Poly(*p*-phenylene vinylene) (PPV)–silica composite thin films were prepared via the sol–gel process incorporating a water-soluble PPV precursor. After solvent evaporation, the spin-coated or quiescently cast films were cured and the PPV precursor and the silica sol were completely converted into the PPV–silica composites. Quiescently cast films show an improved wave-guiding behaviour with a χ^3 value only slightly smaller than pure PPV films. Their structure consists of a nanophase-separated morphology composed of amorphous silica and paracrystalline PPV. Small-angle X-ray scattering and bright field transmission electron microscopy images indicate a random arrangement of the nanoscale domains with average domain size of approximately 4 nm. In contrast, spin-coated films show clusters and cluster–cluster aggregates approximately 100 nm in diameter. The clusters consist of particulate silica and pores, each about 3 nm in size, with the PPV contained in the pores and between the clusters. The observed morphologies are related to film preparation conditions in terms of sol–gel processing, taking the presence of the polymer into account.

(Keywords: poly(*p*-phenylene vinylene); sol–gel; composites)

INTRODUCTION

Polymer sol–gel composite or hybrid materials attract special interest because they combine the beneficial properties of both materials, the polymer and the silica. For example, the excellent optical quality of glass in terms of transparency and wave-guiding can be combined with special non-linear-optical properties of conjugated polymers[1]. In other applications, efforts have been made to combine the high tensile strength and toughness of ordered rigid-rod polymers and the excellent compressive strength of glass[2–4], or to prepare new contact lens materials by the sol–gel procedure employing poly(methyl methacrylate) (PMMA)[5]. The properties of transparent silica–PMMA composites, e.g. density, refractive index, modulus of rupture, compressive strength, abrasion rate and Vickers hardness, have been investigated over a range of 100% silica to 100% PMMA[6]. Material properties are expected to be a function of the number of groups on a polymer chain which react with the silica particles[7]. Experiments showing a decreasing small-angle X-ray scattering (SAXS)-derived correlation length with an increasing number of functional groups on the polymer chain led Huang *et al.*[7] to suggest a model in which all functional groups are connected to clusters formed by silica particles.

To date, there are no publications dealing primarily with the structure and morphology of polymer–silica composites; in particular, there are no investigations utilizing transmission electron microscopy (TEM) or scanning electron microscopy (SEM). In contrast, the microstructure of pure sol–gel processed silica[8] has been extensively investigated by wide-angle X-ray scattering (WAXS)[9], SAXS[10,11], small-angle neutron scattering (SANS)[12,13], TEM[14–17] and SEM[18]. In addition, silica samples have been used as models for fractals [19,20], with various simulations of cluster growth and aggregation of silica[21]. Depending on the sol–gel preparation conditions, many types of structures and morphologies are reported: linear or branched polymers; clusters and diffusion-limited aggregates; fully dense particles. The conditions necessary to form sheets and coatings from sols have been defined[22] and the influences of fast solvent evaporation and the flow conditions in the sol during thin film preparation are reported[23].

In the present work, poly(*p*-phenylene vinylene) (PPV)–silica composites were prepared to combine the excellent optical wave-guiding behaviour of silica with the high third-order non-linear susceptibility, χ^3, of PPV. The structure and morphology of such composite films are expected to influence the optical quality dramatically. The wave-guiding behaviour of the composites can be

* To whom correspondence should be addressed
† Present address: Institute of Physical and Chemical Research (RIKEN), Frontier Research Program, 2-1 Hirosawa, Wako, Saitama 351-01, Japan

0032-3861/93/224607-06

improved, compared to pure PPV, by incorporating the silica phase, whereas the χ^3 value is expected to be reduced only by decreased number density of PPV molecules in the composite. To enhance the waveguiding, the domain sizes of the phases need to be much smaller than the wavelength in order to provide a homogeneous index of refraction to minimize light scattering. The parameters of the sol–gel process and the influence of the film preparation techniques on the structures and morphologies in the PPV–silica composite thin films are investigated in this paper.

EXPERIMENTAL

Sample preparation

Thin films of PPV–silica composites were prepared from a PPV–silica precursor solution using the sol–gel process according to a procedure developed by Prasad *et al.*[24]. This involves the addition of 1 mol% formic acid (relative to tetramethoxysilane (TMOS)) to equal volumes of TMOS, methanol and a 4% solution of poly(*p*-xylylene-α-cyclobutylsulfonium chloride), i.e. PPV precursor, in water under constant agitation. The solution, with pH of about 2–3, was agitated at 60°C for 30 min to form a sol. After cooling to room temperature, eight volumes of MeOH and a defined amount of PPV precursor/H_2O solution were added so that a final mass ratio of PPV:TMOS = 1 was reached. The solution was clarified by treatment in an ultrasonic bath. Upon leaving the solution at room temperature, gelation occurred after 8 h. Our films were prepared by ageing the solution for 4 h. The sol was either spin-coated onto plain or carbon-covered glass slides or quiescently cast onto hydrophobic glass slides or Teflon sheets.

Spin coating was performed by completely covering 75 mm × 25 mm carbon-coated glass slides with 1–2 mm of a thin film of the viscous sol, and subsequently rotating it at 5000 rev min^{-1} for 1 min. Quiescently cast films were prepared by spreading the sol onto a Teflon sheet surrounded by Teflon edges and covering it with a beaker for slow solvent evaporation.

Subsequent to both spin-coated and quiescently cast film formation, the remaining solvent was removed under vacuum at 70°C for about 4 h followed by curing the films at 120°C for 10 h. Finally, the PPV precursor was completely converted into PPV by further heating the films at 200°C for 4 h. Assuming a fully dense film, samples are approximately 50 wt% PPV.

Quiescently cast free-standing films, about 10 μm thick, were embedded in epoxy resin and cut into sections about 50 nm thick using a Reichert–Jung FC-4E microtome at room temperature. Samples spin coated onto carbon film were floated off from glass slides onto a 1 vol% HF/H_2O solution and then picked up with electron microscope grids. Some of the samples were exposed to OsO_4 vapour for 1, 2, 4 and 6 h to possibly selectively stain one of the phases and achieve better TEM image contrast. Other samples were floated onto HF/H_2O solution, with varying concentration of 1–10 vol%, and left there for times varying from 5 to 45 min to study HF etching effects on the PPV–silica composite films.

WAXS was carried out using a Statton camera and recording patterns on Kodak X-ray film. A Kratky camera with flight path, sample holder and detector in a vacuum chamber was utilized for SAXS. X-ray experiments were carried out at 40 kV and 20 mA using Cu-Kα radiation. SAXS data were corrected for background and desmeared. A Jeol 200 CX microscope was operated at 200 kV for bright-field imaging and electron diffraction. Electron diffraction patterns and bright-field images were recorded on Kodak SO-163 film developed for 5 min at 20°C in D 19 full strength developer.

RESULTS AND DISCUSSION

The sol–gel preparation process used for the PPV–silica composites may lead to a structure and morphology which can be anticipated from prior results reported for pure silica samples[8]. A starting solution with pH of 2–3 usually produces small, weakly branched polymeric silica particles. Highly dense particles are not observed in acid solution. The high ratio of water molecules to TMOS ($r = 9$) would enhance the branching. The expected particle diameter in a pure silica film prepared under our conditions[8] is about 5 nm. The gelation time at pH = 2–3 is expected to be very long (100 h). Adding the additional MeOH and PPV precursor solution in the second process step slightly raises the pH and reduces the gelation time. Solidification of the films is significantly influenced by the solvent evaporation rate as the solution is spin-coated or quiescently cast before the gelation point is reached.

Quiescently cast films

WAXS on a stack of 10 free-standing films totalling about 80 μm thickness shows four broad rings (*Figures 1a, b*). The very intense, broad ring at a spacing of about 0.42 nm occurs at the location of the amorphous halo ($d = 0.42$ nm) of silica[9] and the 110 ($d = 0.428$ nm) and the 200 ($d = 0.395$ nm) reflections of PPV (*Table 1*). Two weaker diffraction rings are observed at higher angles at spacings of 0.314 nm and 0.213 nm, which correspond to the 210 and the 220 reflections of PPV according to the structure proposed by Granier *et al.*[25,26]. This indicates that part of the diffuse 0.42 nm ring is due to a contribution of the 110 and 200 PPV reflections. Electron diffraction of microtomed sections of free-standing film show patterns very similar to the WAXS patterns observed on as-prepared free-standing films. Upon high electron irradiation, the weak crystalline PPV rings fade, leaving only the strong 0.42 nm amorphous halo. The diffraction data suggest a two-phase structure consisting of paracrystalline PPV and amorphous silica.

SAXS measurements performed on quiescently cast free-standing films displayed a broad peak ranging over spacings from 2 to 5 nm with a weak maximum around

Table 1 *d*-Spacings (nm) of PPV–silica composite thin films from X-ray diffraction

hkl	Calculated for PPV[a]	Found for PPV/silica
110	0.427	0.42
200	0.395	0.42
210	0.312	0.314
310	0.234	–
220	0.214	0.213
001	0.552	–
021	0.301	–
012	0.329	–

[a] Spacings based on a monoclinic unit cell[27] with $a = 0.709$, $b = 0.605$, $c = 0.658$, $\alpha = 123°$

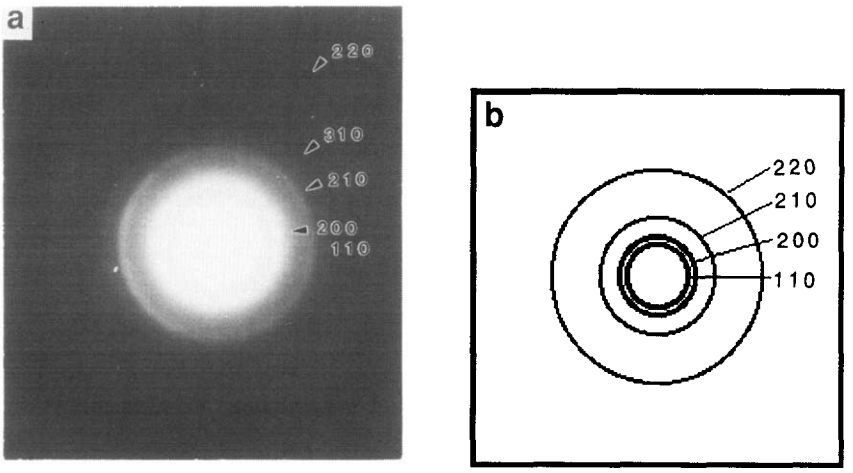

Figure 1 (a) WAXS pattern obtained from a stack of 10 quiescently cast free-standing PPV–silica composite films. (b) Schematic indicating the location of four diffraction rings with spacings of $d = 0.428$, 0.395, 0.314 and 0.213 nm

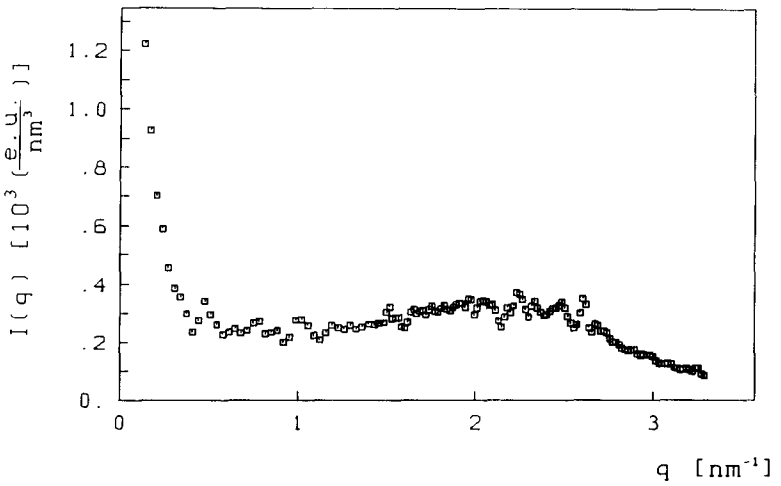

Figure 2 SAXS pattern taken from quiescently cast free-standing PPV–silica composite films at normal beam incidence. A broad peak with a maximum around $d = 3.5$ nm is observed

3.5 nm (*Figure 2*). The strong upturn in the low-angle scattering can be attributed to micropores which also likely account for the strong low-angle scattering evident in the WAXS pattern in *Figure 1a*. The broad SAXS reflection may be related to the average interdomain spacing of the silica and the PPV phases. The broadness of the peak indicates a wide distribution of domain size and a lack of regular packing.

Bright-field TEM images of 50 nm thick microtomed sections of quiescently cast free-standing film show bright regions representing 2-dimensional projections of non-silica regions in a silica matrix, i.e. empty pores or pores filled with PPV (*Figure 3*). No geometrically regular morphology is observed and the low image contrast is consistent with a statistical phase distribution with dimensions much smaller than the thickness of the microtomed sections. The structural detail observed has dimensions smaller than 4 nm, suggesting a random interspersion of silica, pores and PPV. The contrast of the images could not be improved by staining the samples with OsO_4 for various times.

Spin-coated films

Films, about 70 nm thick, spin coated onto carbon-covered glass slides and transferred onto electron microscope grids show clusters and some cluster–cluster aggregates (see *Figure 4a*). The clusters are seen over large parts of the film surface and exhibit diameters between 50 and 100 nm. Higher magnification shows that the clusters consist of pores and particulate silica polymer about 2–3 nm in size (see *Figure 4b*). Similar cluster morphologies have been observed previously by several authors for pure silica sols coated onto carbon-covered grids[15]. All spin-coated samples that were floated off the glass slides onto HF/H_2O solutions of varying concentration or onto pure water show the same morphology, indicating that the morphology is *not* induced by preferential etching of the HF/H_2O solution. Therefore, the carbon film between the composite and the solution can be considered as a protecting layer, as direct contact with concentrated HF/H_2O solution attacks the PPV–silica films.

The cluster morphology observed may arise as a relic related to phase separation between the silica clusters and the PPV precursor solution during the spin-coating process. The fast solvent evaporation during spin coating (seconds or minutes) compared to the slow solvent evaporation during quiescent casting (hours or days) leads to a rapid increase in concentration, which results in a reduced amount of crosslinking between the

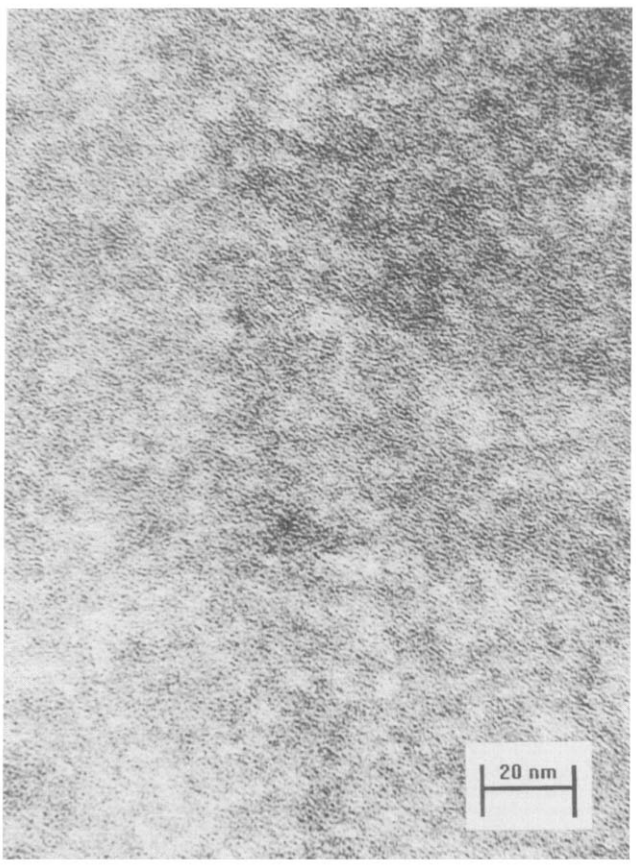

Figure 3 Bright-field image of a microtomed section of a quiescently cast free-standing film. The low contrast and the heterogeneous morphology indicate a statistical distribution of both phases with a domain size smaller than 4 nm

polymeric silica chains. Therefore, silica clusters with a small pore size are formed and solidification is expected to occur before the gel point is reached. In sol–gel films consisting only of pure silica, further solvent evaporation leads to cluster–cluster aggregation and film collapse, which generates porosity. In the composite sol–gel films, the PPV precursor remains in the pores and in between the clusters and seems to prevent aggregation, as mainly single clusters are observed (see *Figure 4a*). This results in a morphology of the PPV–silica spin-coating composites consisting of silica clusters containing some PPV in the porous regions embedded in a PPV matrix. In contrast, the moderate solvent evaporation rate during quiescent casting of the films increases the concentration of the silica and PPV precursor in the sol very slowly, and favours crosslinking between the reactive silica intermediates. Highly branched silica polymer is expected to be formed, resulting in gelation before the solvent evaporates completely. Further ageing leads to the formation of a continuous silica network entrapping the PPV precursor. The formation of a gel mainly by crosslinking reactions thus results in a morphology with a more homogeneous and finer scale phase distribution.

In addition, the possible formation of covalent linkages between the silica gel and the PPV molecules must be considered. The PPV precursor polymer, i.e. poly(*p*-xylylene-α-cyclobutylsulfonium chloride), is not expected to react with TMOS or intermediate products formed during the sol–gel process. However, the available PPV precursor material always contains some molecular structure variations, such as monomer units already

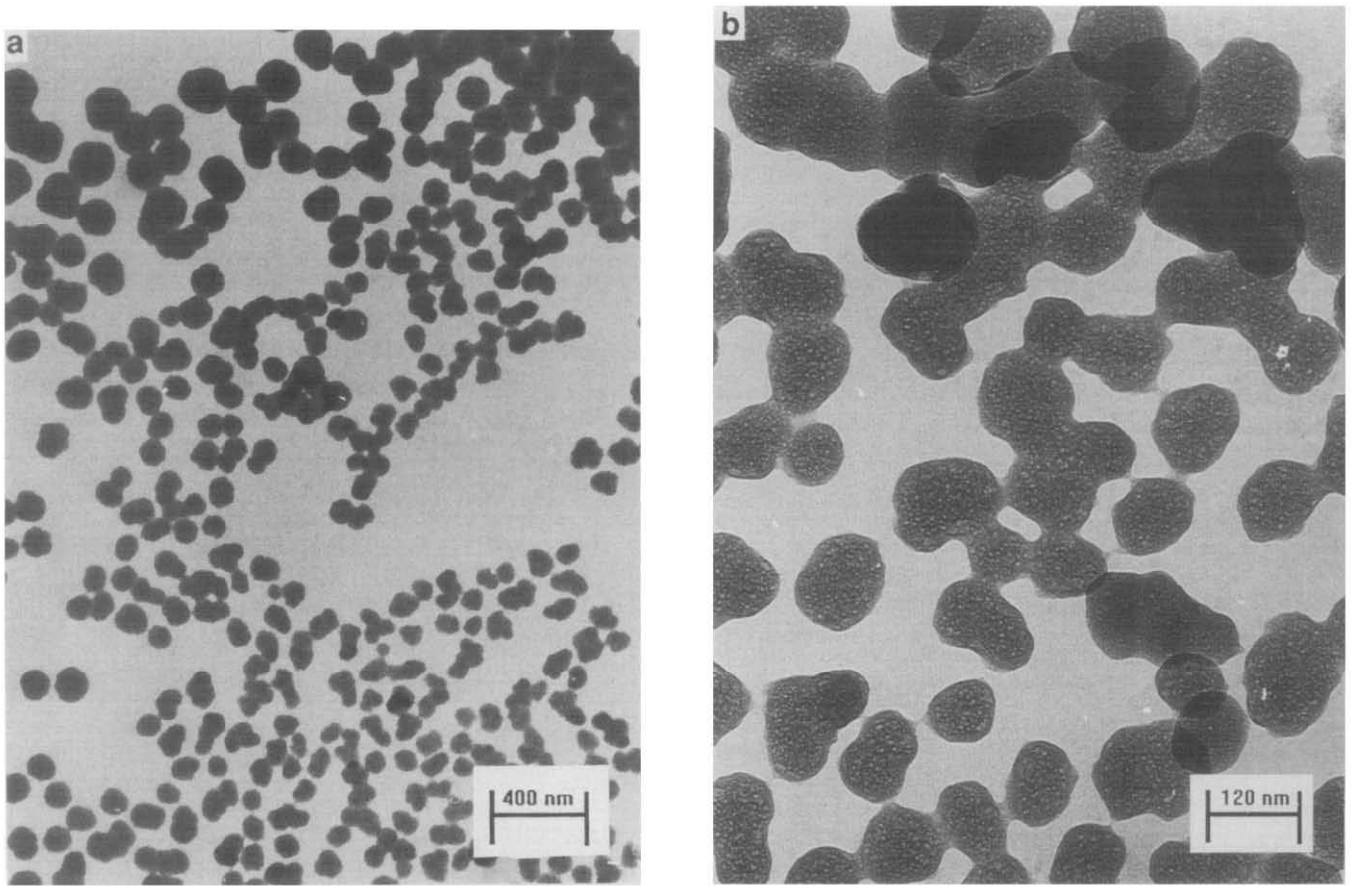

Figure 4 (a) Bright-field image of spin-coated PPV film. Large clusters and cluster–cluster aggregates of silica particles are observed. (b) Higher magnification bright-field image of clusters showing silica particles and pores with dimensions of about 3 nm

converted into phenylene vinylene and chlorine or sulfide-substituted *p*-xylylene units based on elimination and substitution reactions of the sulfonium group[27]. In addition, methoxy-substituted *p*-xylylene units can be formed under acid conditions when methanol is present as a solvent[28,29]. As the sol–gel process is carried out in a mixture of water and methanol under acid conditions, the formation of such monomer units must be considered. Methoxy groups, as well as the double bond in already formed phenylene vinylene units, may react with intermediates formed during the sol–gel process resulting in covalent linkages between both phases. The formation of such linkages could promote compatibility of both phases and influence the phase size. More detailed studies are necessary to investigate the potential reaction of such functional sites, starting, for example, with pure poly(-α-methoxy-*p*-xylylene) or with a precursor already partially converted to PPV and following the influence of the density of functional groups on the resulting film morphology.

Optical properties of quiescently cast films

The linear and non-linear-optical properties of the composite materials were investigated using films several micrometres thick quiescently cast onto glass substrates using the doctor-blading technique[24]. In a planar wave-guide configuration, both the prism and the grating coupling methods were used to determine the wave-guiding behaviour. Low optical losses related to scattering confirmed that the domain sizes were significantly smaller than the optical wavelength. Using prism coupling, propagating distances of more than 2 cm at a wavelength of 1.06 μm were readily achieved for the TE modes, indicating optical losses of less than 2 db cm^{-1}. Such a value represents more than a tenfold improvement in the optical wave-guiding behaviour compared to pure PPV films.

The excellent optical quality of these composite films allowed investigations of third-order non-linear-optical properties of the composite films using a variety of techniques, such as femtosecond transient absorption, optical Kerr gate and degenerate four-wave mixing, as reported in more detail elsewhere[30]. The results discussed here were obtained using degenerate four-wave mixing with 400 femtosecond pulses[31]. The χ^3 value of 3×10^{-10} esu, obtained for the PPV–silica composites at a wavelength of 602 nm and with the response time limited to the laser pulse width, is only slightly smaller than the maximum value of about 4×10^{-10} esu reported by Singh *et al.*[31] for pure stretched PPV samples (draw ratio 10:1) with all polarizations of the incident beams parallel to the stretching direction. Based on the number density consideration, a reduction in the χ^3 value by a factor of at least 1.6 is expected for a composite film containing about 50 wt% PPV. Taking into account that the PPV molecules exhibit a paracrystalline phase with random crystallite orientation in the PPV–silica composites, an additional reduction of the χ^3 value by a factor close to three is expected, resulting in an estimated χ^3 value of approximately 1×10^{-10} esu. The fact that the χ^3 value observed for the composite film is much closer to the value observed for the pure PPV film, may be a consequence of the significantly improved optical quality of the composite films, permitting a more realistic assessment of the intrinsic χ^3 value of PPV. A similar observation was made in a polymer composite of poly(*p*-phenylene-benzbisthiazole) and aromatic, amorphous nylon, where the improved optical quality of the film also yielded a higher χ^3 value[32].

CONCLUSIONS

Thin films of PPV–silica composites were prepared from a PPV–silica precursor solution using the sol–gel process and spin coating or quiescently casting the sol onto solid substrates prior to the gel point.

The observed morphologies of the quiescently cast and the spin-coated films can be related to the parameters and conditions of the sol–gel procedure, taking into account the presence of the PPV precursor polymer in the solution. The sol–gel, quiescently cast PPV–silica composite film process is an excellent approach to prepare thin films with a high non-linear-optical coefficient χ^3 and a significantly improved wave-guiding behaviour compared to pure PPV films.

Quiescently cast PPV–silica composite thin films (1:1 mass ratio) show improved wave-guiding behaviour with optical losses of less than 10 db cm^{-1} and a χ^3 value of 3×10^{-10} esu, only slightly smaller than the value observed for pure PPV samples. The χ^3 value observed on the composite films is much higher than expected considering the number density of PPV units and the random orientation of the PPV molecules in the composite.

The excellent optical properties of the composite films are due to a nanophase separated morphology consisting of a statistically distributed amorphous silica phase and a paracrystalline PPV phase with maximum domain sizes of less than about 4 nm. In contrast, spin-coated PPV–silica composite films show a morphology consisting of clusters with dimensions between 50 and 100 nm formed by silica particles and pores, both about 2 to 3 nm in size, embedded in a PPV film. The PPV precursor matrix between the silica clusters prevents cluster–cluster aggregation during the rapid solvent evaporation so that mainly single clusters are observed.

ACKNOWLEDGEMENTS

This work was supported by the Center of Materials Science and Engineering at the Massachusetts Institute of Technology, NSF grant DMR 9022933 and grant AFOSR 91-0078 from the Air Force Office of Scientific Research. The work at State University of New York at Buffalo was supported by the Office of Innovative Science and Technology — Defense Initiative Organization, Air Force Office of Scientific Research through contract number F49620-91-C0053.

REFERENCES

1 Wung, C. J., Pang, Y., Prasad, P. N. and Karasz, F. E. *Polymer* 1991, **32**, 605
2 Philipp, G. and Schmidt, H. *J. Non-Cryst. Solids* 1984, **63**, 283
3 Kovar, R. F. and Lusignea, R. W. *Mater. Res. Soc. Symp. Proc.* 1988, **121**, 755
4 Jaffe, M. and Sawyer, L. C. in 'Ultrastructure Processing of Advanced Ceramics' (Eds J. D. Mackenzie and D. R. Ulrich), Wiley, New York, 1988, p. 725
5 Mark, J. E. in 'Ultrastructure Processing of Advanced Ceramics' (Eds J. D. Mackenzie and D. R. Ulrich), Wiley, New York, 1988, p. 623

6 Pope, E. J. A., Asami, M. and Mackenzie, J. D. *J. Mater. Res.* 1989, **4**, 1018
7 Huang, H. H., Wilkes, G. L. and Carlson, J. G. *Polymer* 1989, **30**, 2002
8 Brinker, C. J. and Scherer, G. W. in 'Sol–Gel Science, The Physics and Chemistry of Sol–Gel Processing', Academic Press, London, 1990, p. 97
9 Warren, B. E. and Biscoe, J. *J. Am. Ceram. Soc.* 1938, **21**, 49
10 Keefer, K. D. *Mater. Res. Soc. Symp. Proc.* 1984, **32**, 15
11 Schaefer, D. W. and Keefer, D. *Mater. Res. Soc. Symp. Proc.* 1984, **32**, 1
12 Ramsay, D. F. *Chem. Soc. Rev.* 1986, **15**, 335
13 Ramsay, D. F. and Booth, B. O. *J. Chem. Faraday Trans.* 1983, **1**, 173
14 Mulder, C. A. M., Leeuwen-Stienstra, G. and Lierop, J. G. *J. Non-Cryst. Solids* 1986, **82**, 148
15 Stoeber, W., Fink, A. and Bohn, E. *J. Colloid Interface Sci.* 1986, **26**, 62
16 Komareni, S., Breval, E. and Roy, R. *J. Non-Cryst. Solids* 1986, **79**, 195
17 Nogami, M. and Moriya, Y. *J. Non-Cryst. Solids* 1980, **37**, 191
18 Lecloux, A. J., Bronckart, J., Noville, F., Dodet, C., Marchot, P. and Pirard, J. P. *Colloids and Surfaces* 1986, **19**, 359
19 Mandelbrot, B. B. 'Fractals, Form, Chance, and Dimension', W. H. Freeman, San Francisco, 1977
20 Martin, J. E. and Hurd, A. J. *J. Appl. Cryst.* 1987, **20**, 61
21 Meakin, P. *Phys. Rev. Lett.* 1983, **51**, 1119
22 Sakka, S., Kamyia, K., Makita, K. and Yamamoto, Y. *J. Non-Cryst. Solids* 1984, **63**, 223
23 Brinker, C. J. and Scherer, G. W. in 'Sol–Gel Science, The Physics and Chemistry of Sol–Gel Processing', Academic Press, London, 1990, p. 787
24 Prasad, P. N., Karasz, F. E., Pang, Y. and Wung, C. J. US Patent Number 5,130,362, 1992
25 Granier, T., Thomas, E. L., Gagnon, D. R., Karasz, F. E. and Lenz, R. W. *J. Polym. Sci.: Part B: Polym. Phys.* 1986, **24**, 2793
26 Masse, M. A. PhD Thesis, University of Massachusetts, 1989
27 Lenz, R. W., Han, C. C., Stenger-Smith, J. and Karasz, F. E. *J. Polym. Sci., Polym. Chem. Edn* 1988, **26**, 3241
28 Momii, T., Tokito, S., Tsutsui, T. and Saito, S. *Chem. Lett.* 1988, 1201
29 Burn, P. L., Bradley, D. D. C., Friend, A. R. and Holmes, A. B. *Synth. Met.* 1991, **261**, 41
30 Pang, Y., Samoc, M. and Prasad, P. N. *J. Chem. Phys.* 1991, **94**, 5282
31 Singh, B. P., Prasad, P. N. and Karasz, F. E. *Polymer* 1988, **29**, 1940
32 Lee, C. Y.-C., Swiatkiewicz, J., Prasad, P. N., Mehta, R. and Bai, S. J. *Polymer* 1991, **32**, 1195